


## Heterogeneous traffic flow modeling with drivers' timid and aggressive characteristics

Cong Zhai(翟聪), Weitiao Wu(巫威眺), and Songwen Luo(罗淞文)
**Citation:**Chin. Phys. B, 2021, 30 (**10**): 100507. DOI: 10.1088/1674-1056/abf7ae
Journal homepage: http://cpb.iphy.ac.cn; http://iopscience.iop.org/cpb

**What follows is a list of articles you may be interested in**

---

## Collective motion of polar active particles on a sphere

Yi Chen(陈奕), Jun Huang(黄竣), Fan-Hua Meng(孟繁华), Teng-Chao Li(李腾超), and Bao-Quan Ai(艾保全)
Chin. Phys. B, 2021, 30 (**10**): 100510. DOI: 10.1088/1674-1056/abfccf

## Dynamic modeling and aperiodically intermittent strategy for adaptive finite-time synchronization control of the multi-weighted complex transportation networks with multiple delays

Ning Li(李宁), Haiyi Sun(孙海义), Xin Jing(靖新), and Zhongtang Chen(陈仲堂)
Chin. Phys. B, 2021, 30 (**9**): 090507. DOI: 10.1088/1674-1056/abea92

## Identification of unstable individuals in dynamic networks

Dongli Duan(段东立), Tao Chai(柴涛), Xixi Wu(武茜茜), Chengxing Wu(吴成星), Shubin Si(司书宾), and Genqing Bian(边根庆)
Chin. Phys. B, 2021, 30 (**9**): 090501. DOI: 10.1088/1674-1056/abe92f

## Lagrangian analysis of the formation and mass transport of compressible vortex rings generated by a shock tube

Haiyan Lin(林海燕), Yang Xiang(向阳, Hong Liu(刘洪), and Bin Zhang(张斌)
Chin. Phys. B, 2021, 30 (**3**): 030501. DOI: 10.1088/1674-1056/abc67f

## Solid angle car following model

Dongfang Ma(马东方), Yueyi Han(韩月一), Sheng Jin(金盛)
Chin. Phys. B, 2020, 29 (**6**): 060504. DOI: 10.1088/1674-1056/ab862c

---

# Heterogeneous traffic flow modeling with drivers' timid and aggressive characteristics*

Cong Zhai(翟聪)[1,2], Weitiao Wu(巫威眺)[1,†], and Songwen Luo(罗淞文)[1]

[1] School of Civil Engineering and Transportation, South China University of Technology, Guangzhou 510641, China
[2] School of Transportation and Civil Engineering and Architecture, Foshan University, Foshan 528000, China

(Received 10 January 2021; revised manuscript received 7 April 2021; accepted manuscript online 14 April 2021)

The driver's characteristics (e.g., timid and aggressive) has been proven to greatly affect the traffic flow performance, whereas the underlying assumption in most of the existing studies is that all drivers are homogeneous. In the real traffic environment, the drivers are distinct due to a variety of factors such as personality characteristics. To better reflect the reality, we introduce the penetration rate to describe the degree of drivers' heterogeneity (i.e., timid and aggressive), and proceed to propose a generalized heterogeneous car-following model with different driver's characteristics. Through the linear stability analysis, the stability conditions of the proposed heterogeneous traffic flow model are obtained based on the perturbation method. The impacts of the penetration rate of drivers with low intensity, the average value and standard deviation of intensity parameters characterizing two types of drivers on the stability of traffic flow are analyzed by simulation. Results show that higher penetration of aggressive drivers contributes to traffic flow stability. The average value has a great impact on the stability of traffic flow, whereas the impact of the standard deviation is trivial.

**Keywords:** heterogeneous car-following model, driver characteristic, penetration rate, stability

**PACS:** 05.60.−k, 45.70.Vn **DOI:** 10.1088/1674-1056/abf7ae

## 1. Introduction

Traffic congestion and emission are the major issues in the transportation engineering. The growing number of ridership results in unprecedented advances in traffic management technology, such as public transit operational strategies[1–3] and transportation electrification.[4] A good understanding of driving behavior and traffic flow can also benefits the transportation planning and control. This raises a distinct line of research on the traffic flow modeling in an aim to analyze the formation and propagation mechanism of traffic congestion.

Methodologically, traffic flow models can be grouped into two categories: microscopic models and macroscopic models. The former group is represented by car following models[5–10] and cellular automaton models,[11–13] while the latter is represented by continuous flow models[14–19] and lattice hydrodynamics models.[20–27] Different to microscopic models, the macroscopic models take the traffic flow as a compressible continuous fluid composed of a number of vehicles, of which the simulation time is indifferent to the number of vehicles. However, the macroscopic models cannot capture the interactions among vehicles and the resulting microscopic driving behaviors. In comparison, the microscopic models take individual vehicles as the research object, which facilitates the analysis of driving behaviors of each vehicle. Given these advantages, the microscopic traffic flow models have promoted rapidly in the transportation research community over the past decades.

In 1995, Bando *et al.*[28] proposed a seminar work of single-lane car-following model. This work is a stimulus-response model, where the stimulus source is the difference between the real-time speed and the optimal speed of the target vehicle. As opposed to previous microscopic traffic flow models, this model introduced the optimal velocity function with inflection points, enabling to perform linear and nonlinear stability analysis to obtain kink–anti-kink solitary waves. Since then, this model has been widely applied in the field of traffic flow research, especially in traffic physics, and a number of extended models have been given. For example, Zhang and Tang[29] proposed a car-following model accounting for the preceding car's taillight, which showed that the taillight effect can improve the traffic flow stability and enhance the safety. Jin and Cheng[30] considered the effect of the optimal velocity changes with memory in the car-following model. Li *et al.*[31] incorporated the time-varying reaction time delay of the drivers in the car-following model, and designed a robust state feedback control strategy to suppress the traffic jam. Li *et al.*[32] presented a car-following model for electronic vehicle traffic flow to minimize the energy consumption. Table 1 provides an overview of the extended models of the traditional optimal velocity car-following model.

*Project supported by the Regional Joint Fund for Foundation and Applied Research Fund of Guangdong Province, China (Grant No. 2019A1515111200), Youth Innovation Talents Funds of Colleges and Universities in Guangdong Province, China (Grant No. 2018KQNCX287), the Science and Technology Program of Guangzhou, China (Grant No. 201904010202), the National Science Foundation of China (Grant No. 72071079), and the Science and Technology Program of Guangdong Province, China (Grant No. 2020A1414010010).

†Corresponding author. E-mail: ctwtwu@scut.edu.cn

© 2021 Chinese Physical Society and IOP Publishing Ltd 

**Table 1.** Research overview of optimal velocity car-following model.

| Authors | Characteristics | References |
|---|---|---|
| Guo and Zhang | multiple preceding speed difference | [33,34] |
| Li | multiple headway, velocity and acceleration difference | [35] |
| Yu, Ge and Zhu | delay effect | [36–38] |
| Cao, Wang and Liu | memory effect | [39–41] |
| Peng, Zhang, Cheng and Zhou | anticipation (forecast) time effect | [42–45] |
| Tang | driver's attribution | [46] |
| Peng, Cheng and Sharma | timid and aggressive driving behaviors | [47–50] |
| Wang and Tang | driver's bounded rationality | [51,52] |
| Tang | ramp effect | [53] |
| Ge | two-lane effect | [54] |
| Li | non-lane discipline | [55–57] |
| Wang | cyberattacks | [58] |
| Sun and Li | electronic throttle opening angle | [59,60] |
| Yu | cooperative adaptive cruise control | [61] |
| Li, Jin and Cheng | control method | [62–64] |

Although a variety of factors have been investigated in the car-following models, most of the extant studies primarily focused on one single type of drivers and vehicles, underlying that the drivers are homogeneous. However, in the real traffic environment, the driving behaviors are heterogeneous in the presence of different driver's characteristics, such as the age, gender, and vehicle types. There are only a handful of works that investigate the heterogeneous traffic flow. At the micro level, Yang *et al.*[65] developed a car–truck cellular automata model considering the difference in safety distance, reaction time and randomization probability. Li *et al.*[66] presented a cellular automata traffic flow model considering the differences in acceleration and delay probabilities of different types of vehicles. Literatures[67–70] introduced the differences in driver's sensitivity, anticipation driving behavior and maximum and minimum speed and driver's psychological headway of different types of vehicles into the optimal velocity car-following model. At the macro level, considering that the difference of electronic throttle angle between different types of vehicles and the psychological headway between different types drivers, two heterogeneous continuous flow models were proposed in literatures.[71,72] As pointed out by literatures,[47–50] the driving style can be roughly divided into two types: aggressive and timid, based on the prevalent driving behavior. The former group of drivers with skillful driving capability speed up by taking advantage of predicted traffic state, while the latter group is risk aversion and more prudent in acceleration. Although the driver's characteristics (e.g., timid and aggressive) is a proven contributor to the traffic flow performance, the underlying assumption in most of the extant studies is that all drivers are homogeneous (see our analysis in Section 2). In the real traffic environment, the drivers are distinct due to a variety of factors. Motivated by this fact, in this paper we will construct a new heterogeneous traffic flow model with different driver's characteristics. The heterogeneity is reflected by their personality characteristics (i.e., timid and aggressive) and the corresponding penetration rates. To the best of our knowledge, this is the first time that the effect of timid and aggressive drivers is simultaneously incorporated into the heterogeneous car-following model. This research is expected to provide theoretical insights into the microscopic traffic flow simulation and traffic control.

The structure of this paper is as follows: In Section 2, a new heterogeneous traffic flow model considering different driver's characteristic is given. In Section 3, the stability criterion is obtained through performing a linear stability analysis. In Section 4, the impact of critical parameters is investigated by simulation. The conclusions of the paper and future works are given in Section 5.

## 2. Model

In this section, we will revisit the traditional model and introduce the rationale behind our proposed model. The primary notations used in this paper are listed in Table 2. To analyze the car-following behaviors on a single lane, Bando *et al.*[28] proposed an optimal velocity (OV) model, the motion equation of which is

$$\frac{\mathrm{d}v_n(t)}{\mathrm{d}t} = a\left[V\left(y_n(t)\right) - v_n(t)\right], \tag{1}$$

where $y_n(t)$ is determined by the following expression:

$$\frac{\mathrm{d}y_n(t)}{\mathrm{d}t} = v_{n+1}(t) - v_n(t). \tag{2}$$

In Eq. (1), $V(\cdot)$ is expressed as

$$V(y) = \frac{v_{\max}}{2}\left[\tanh\left(y - h_{\mathrm{c}}\right) + \tanh\left(h_{\mathrm{c}}\right)\right]. \tag{3}$$

Following the literature,[28] we have $v_{\max}=2$, and $h_{\mathrm{c}}=4$.

Later, Helbing and Tilch[73] carried out the parameter tuning on the OV model based on the measured data. They found that the acceleration of the vehicle is too large and the deceleration is unreasonable, such that the collisions may even occur.

For this reason, they proposed that the influence of the speed difference should be included when the current vehicle speed is lower than the following vehicle. As a result, the general force (GF) model is given, specifically,

$$\frac{\mathrm{d}v_n(t)}{\mathrm{d}t} = a\left[V\left(y_n(t)\right) - v_n(t)\right] + kH\left(-v_n(t)\right)\Delta v_n(t), \quad (4)$$

where $\Delta v_n = v_{n+1}(t) - v_n(t)$, $H(\cdot)$ is the Heaviside function, specifically,

$$H(x) = \begin{cases} 0, & x \le 0, \\ 1, & x > 0. \end{cases} \quad (5)$$

Jiang *et al.*[74] used the above GF model to simulate the start-up process of a stationary vehicle and found that the starting wave speed of the traffic flow was too small. Given this fact, they proposed that the effect of speed difference should be considered when the current vehicle speed was greater than the following vehicle. Consequently, the full velocity difference (FVD) model was presented, and the formulation is expressed as follows:

$$\frac{\mathrm{d}v_n(t)}{\mathrm{d}t} = a\left[V\left(y_n(t)\right) - v_n(t)\right] + k\Delta v_n(t). \quad (6)$$

As mentioned previously, the driving styles are affected by a variety of factors such as personality characteristics and driving years. Generally, the drivers exhibit two types of driving styles, i.e., aggressive and timid characteristics. When the aggressive characteristics dominate, the external performance of drivers will be aggressive. To pursue a faster driving speed, aggressive drivers will predict the next time step traffic situation based on their experience and use the forecast traffic information to adjust the vehicle speed. On the contrary, when the timid characteristics dominate, the drivers are inclined to use the traffic state at the last moment to adjust the vehicle acceleration. Based on this, Peng *et al.*[47] presented a homogeneous car-following model by incorporating the timid and aggressive driving behaviors. The motion equation is specified as follows:

$$\begin{aligned}\frac{\mathrm{d}v_n(t)}{\mathrm{d}t} = {} & a\big[pV\left(y_n(t+\alpha_1\tau)\right) + (1-p)V\left(y_n(t-\alpha_2\tau)\right) \\ & - v_n(t)\big] + k\Delta v_n(t), \end{aligned} \quad (7)$$

where the values of prediction time and delay time can be obtained through traffic survey. To ease the subsequent analysis, we assume $\alpha_1 = \alpha_2 = \alpha$. When $0 \le p < 1/2$ ($1/2 < p \le 1$), the drivers are timid (aggressive). Typically, when $p = 0$ or $p = 1$, the drivers are the totally timid or aggressive, respectively.

**Remark 1** According to Eq. (7), the driver characteristics of the $n$-th car are also determined by the parameter $p$, $\alpha_1$, and $\alpha_2$, whereby the motion equation of the $n$-th car can be given. To analyze the effect of driver's characteristics, previous works[44–48] assumed that the dynamic equations of all vehicles along the road comply with Eq. (7). As such, if the driver of $n$-th vehicle is a timid (aggressive) characteristic, then the remaining drivers on the road are also timid (aggressive), which indicates that all drivers are homogeneous. In this way, different characteristics of each driver are ignored. Since drivers in the real traffic environment are affected by a variety of factors such as age and personality, the above assumption is difficult to defend. In reality, there exist differences among drivers on the road. For example, both aggressive drivers and timid drivers coexist on the road. Even if all drivers on the road are of the same type (i.e., all drivers are timid or aggressive), some personality differences still exist. The distinctions are mainly reflected by the difference of parameter $p$ in Eq. (7).

**Table 2.** Primary notations used in the proposed model.

| Symbols | Definition | Unit |
|---|---|---|
| $n$ | the subscript of vehicles | - |
| $a$ | driver's sensitivity | $\mathrm{s}^{-1}$ |
| $y_n(t)$ | instantaneous headway information | m |
| $v_n(t)$ | instantaneous velocity information | $\mathrm{m}\cdot\mathrm{s}^{-1}$ |
| $V(\cdot)$ | optimal speed function | $\mathrm{m}\cdot\mathrm{s}^{-1}$ |
| $v_{\max}$ | maximum speed | $\mathrm{m}\cdot\mathrm{s}^{-1}$ |
| $h_{\mathrm{c}}$ | safety distance | m |
| $\Delta v_n$ | velocity difference information | $\mathrm{m}\cdot\mathrm{s}^{-1}$ |
| $k$ | weight coefficient of velocity difference term | - |
| $\alpha_1\tau$ | delay time corresponding to timid drivers | s |
| $\alpha_2\tau$ | anticipation time corresponding to aggressive drivers | s |
| $p$ | intensity parameter of driver's characteristic | - |
| $p_{\mathrm{h}}$ | high intensity parameter | - |
| $p_{\mathrm{l}}$ | low intensity parameter | - |
| $q$ | penetration rate of drivers with low intensity | - |

Based on the above analysis, we assume that there are two different types of drivers on the road. To this end, we introduce parameter $q$ to represent the heterogeneity between drivers on the road. As a result, an extended traffic flow model with heterogeneous drivers' characteristics is proposed, and the specific expression of the proposed model is given as follows:

$$\begin{aligned}\frac{\mathrm{d}v_n(t)}{\mathrm{d}t} = {} & a\big[p_{\mathrm{l}}V\left(y_n(t+\alpha\tau)\right) + (1-p_{\mathrm{l}})V\left(y_n(t-\alpha\tau)\right) \\ & - v_n(t)\big] + k\Delta v_n(t), \end{aligned}$$

for drivers with lower inensity $p_{\mathrm{l}}$ with a percentage of $q$,

$$\begin{aligned}\frac{\mathrm{d}v_n(t)}{\mathrm{d}t} = {} & a\big[p_{\mathrm{h}}V\left(y_n(t+\alpha\tau)\right) + (1-p_{\mathrm{h}})V\left(y_n(t-\alpha\tau)\right) \\ & - v_n(t)\big] + k\Delta v_n(t), \end{aligned}$$

for drivers with higher inensity $p_{\mathrm{h}}$ with a percentage of $1-q$. (8)

If $q = 0$ or $q = 1$, our heterogeneous traffic flow model collapses into the traditional homogeneous traffic flow model.

**Remark 2** Although the parameter $\alpha$ may vary among different drivers, this study focuses on the impact of different driver's characteristics on traffic flow stability. Therefore, in

the future study we will further analyze the effect of different driving skills on the stability of traffic flow under the same driver's characteristics.

## 3. Linear stability analysis

In this section, we will analyze the stability of the new heterogeneous traffic flow model based on the perturbation method. To facilitate the analysis, we first transform Eq. (8) into the following form:

$$\begin{aligned}\frac{\mathrm{d}v_n(t)}{\mathrm{d}t} &= a\big[p_n V\left(y_n(t+\alpha\tau)\right)+(1-p_n)V\left(y_n(t-\alpha\tau)\right)\\ &\quad -v_n(t)\big]+k\Delta v_n(t).\end{aligned} \tag{9}$$

We assume that the vehicle $n$ runs with a constant speed $v_n^0$ and headway $y_n^0$, where $v_n^0{=}V\left(y_n^0\right)$. Now, a small disturbance is imposed into the steady state, i.e.,

$$y_n(t)=y_n^0+\delta y_n(t),\ \ v_n(t)=v_n^0+\delta v_n(t). \tag{10}$$

Performing Taylor expansion on $V\left(y_n(t+\alpha\tau)\right)$ and $V\left(y_n(t-\alpha\tau)\right)$, ignoring higher-order nonlinear terms, we have

$$\begin{aligned}V\left(y_n(t+\alpha\tau)\right) &= V\left(y_n^0+\delta y_n(t+\alpha\tau)\right)\\ &= V\left(y_n^0\right)+V'\left(y_n^0\right)\delta y_n(t+\alpha\tau),\end{aligned} \tag{11}$$

$$\begin{aligned}V\left(y_n(t-\alpha\tau)\right) &= V\left(y_n^0+\delta y_n(t-\alpha\tau)\right)\\ &= V\left(y_n^0\right)+V'\left(y_n^0\right)\delta y_n(t-\alpha\tau).\end{aligned} \tag{12}$$

Substituting Eqs. (10)–(12) into Eq. (9), we have

$$\begin{aligned}\frac{\mathrm{d}\delta v_n(t)}{\mathrm{d}t} &= a\big[p_n V'\delta y_n(t+\alpha\tau)+(1-p_n)V'\delta y_n(t-\alpha\tau)\\ &\quad -\delta v_n(t)\big]+k\Delta\delta v_n(t),\end{aligned} \tag{13}$$

where $V'=\left.\frac{\mathrm{d}V(y)}{\mathrm{d}y}\right|_{y=y_n^0}$.

Here, we assume that $\delta v_n=V_n\mathrm{e}^{\mathrm{i}nw+\lambda t}$, $\delta y_n=Y_n\mathrm{e}^{\mathrm{i}nw+\lambda t}$, and $\delta\Delta v_n=\Delta V_n\mathrm{e}^{\mathrm{i}nw+\lambda t}$. According to Eq. (2), we can see that

$$Y_n=\frac{\mathrm{e}^{\mathrm{i}w}V_{n+1}-V_n}{\lambda}. \tag{14}$$

Similarly, since $\Delta v_n=v_{n+1}(t)-v_n(t)$, we have

$$\Delta V_n=\mathrm{e}^{\mathrm{i}w}V_{n+1}-V_n. \tag{15}$$

Substituting Eqs. (14) and (15) into Eq. (13), we have

$$\begin{aligned}\lambda V_n &= a\Bigg[\mathrm{e}^{\lambda\alpha\tau}p_nV'\frac{\mathrm{e}^{\mathrm{i}w}V_{n+1}-V_n}{\lambda}\\ &\quad +\mathrm{e}^{-\lambda\alpha\tau}(1-p_n)F'\frac{\mathrm{e}^{\mathrm{i}w}V_{n+1}-V_n}{\lambda}-V_n\Bigg]\\ &\quad +k\left(\mathrm{e}^{\mathrm{i}w}V_{n+1}-V_n\right).\end{aligned} \tag{16}$$

Subsequently, the above formula can be rewritten as follows:

$$\begin{aligned}&V_n\left[\lambda^2+(k+a)\lambda+a\mathrm{e}^{\lambda\alpha\tau}p_nV'+a\mathrm{e}^{-\lambda\alpha\tau}(1-p_n)V'\right]\\ &=\mathrm{e}^{\mathrm{i}w}V_{n+1}\left[\lambda k+a\mathrm{e}^{\lambda\alpha\tau}p_nV'+a\mathrm{e}^{-\lambda\alpha\tau}(1-p_n)V'\right].\end{aligned} \tag{17}$$

Assuming that the number of vehicles along the road is $N$ and the road simulation condition is periodic boundary, that is, $V_{N+1}=V_1$, we can obtain the nontrivial solution of Eq. (17) when $V_n\neq 0$, that is,

$$\begin{aligned}&\prod_{n=1}^{N}\left[\lambda^2+(k+a)\lambda+a\mathrm{e}^{\lambda\alpha\tau}p_nV'+a\mathrm{e}^{-\lambda\alpha\tau}(1-p_n)V'\right]\\ &=\mathrm{e}^{N\mathrm{i}w}\prod_{n=1}^{N}\left[\lambda k+a\mathrm{e}^{\lambda\alpha\tau}p_nV'+a\mathrm{e}^{-\lambda\alpha\tau}(1-p_n)V'\right].\end{aligned} \tag{18}$$

Putting the following expansions $\lambda\approx\lambda_1\mathrm{i}w+\lambda_2(\mathrm{i}w)^2$, $\mathrm{e}^{N\mathrm{i}w}\approx 1+N\mathrm{i}w+\frac{(N\mathrm{i}w)^2}{2!}$, and $\mathrm{e}^{-\lambda\alpha\tau}\approx 1-\lambda\alpha\tau$ into the above formula, the first-order and second-order coefficients of $\mathrm{i}w$ can be obtained as follows:

$$\begin{aligned}\Theta(\mathrm{i}w) &= \lambda_1\sum_{n\in N}\left[k+a+\alpha(2p_n-1)V'\right]\prod_{m\neq n,m\in N}aV'\\ &\quad -N\prod_{n=1}^{N}aV'\\ &\quad -\lambda_1\sum_{n\in N}\left[k+\alpha(2p_n-1)V'\right]\prod_{m\neq n,m\in N}aV'\\ &= 0,\end{aligned} \tag{19}$$

$$\begin{aligned}\Theta\left((\mathrm{i}w)^2\right) &= \lambda_1^2\sum_{n=1}\prod_{m\neq j,m\in N}aV'\\ &\quad +\lambda_2\sum_{n=1}\left[k+a+\alpha(2p_n-1)V'\right]\prod_{m\neq j,m\in N}aV'\\ &\quad +\lambda_1^2\sum_{n<m,(m,n)\in N}\left[k+a+\alpha(2p_m-1)V'\right]\\ &\quad \times\left[k+a+\alpha(2p_n-1)V'\right]\prod_{j\neq(m,n),j\in N}aV'\\ &\quad -\frac{N^2}{2}\prod_{n\in N}aV'\\ &\quad -N\lambda_1\sum_{n\in N}\left[k+\alpha(2p_n-1)V'\right]\prod_{m\neq j,m\in N}aV'\\ &\quad -\lambda_2\sum_{n=1}\left[k+\alpha(2p_n-1)V'\right]\prod_{m\neq j,m\in N}aV'\\ &\quad -\lambda_1^2\sum_{n<m,(m,n)\in N}\left[k+\alpha(2p_m-1)V'\right]\\ &\quad \times\left[k+\alpha(2p_n-1)V'\right]\prod_{j\neq(m,n),j\in N}aV'\\ &= 0.\end{aligned} \tag{20}$$

Solving Eq. (17) yields the formulation

$$\lambda_1=\frac{N}{\sum\limits_{n\in N}\frac{1}{V'}}=V'. \tag{21}$$

Substituting Eq. (19) into Eq. (18), we have

$$\frac{\lambda_2}{\lambda_1^2}\sum_{n=1}\frac{1}{V'} = -\sum_{n=1}\left\{\frac{1}{aV'}-\frac{1}{2}\left(\frac{1}{V'}\right)^2-\frac{k}{a}\left(\frac{1}{V'}\right)^2 -\frac{\alpha(2p_n-1)}{aV'}\right\}. \tag{22}$$

Based on the stability theory, when $\lambda_2 < 0$, the traffic flow is stable. In order to ensure that the above formula holds, based on Eq. (20), we have

$$\sum_{n=1}\left\{\frac{1}{aV'}-\frac{1}{2}\left(\frac{1}{V'}\right)^2-\frac{k}{a}\left(\frac{1}{V'}\right)^2-\frac{\alpha(2p_n-1)}{aV'}\right\}\geq 0. \tag{23}$$

Since there are two different types of drivers along the road, the following in-equation holds:

$$q\left[\frac{1}{aV'}-\frac{1}{2}\left(\frac{1}{V'}\right)^2-\frac{k}{a}\left(\frac{1}{V'}\right)^2-\frac{\alpha(2p_\mathrm{l}-1)}{aV'}\right]+(1-q) \times\left[\frac{1}{aV'}-\frac{1}{2}\left(\frac{1}{V'}\right)^2-\frac{k}{a}\left(\frac{1}{V'}\right)^2-\frac{\alpha(2p_\mathrm{h}-1)}{aV'}\right]\geq 0. \tag{24}$$

Based on Eq. (24), we can obtain the neutral curve of the new heterogeneous model as

$$\begin{aligned} a_\mathrm{s} &= 2V'-2k-2qV'\alpha(2p_\mathrm{l}-1) \\ &\quad -2(1-q)V'\alpha(2p_\mathrm{h}-1). \end{aligned} \tag{25}$$

Typically, when $q=0$ or $q=1$, the following neutral stable curve of the homogeneous traffic flow model can be obtained:

$$\begin{aligned} a_\mathrm{s} &= 2V'-2k-2V'\alpha(2p_\mathrm{h}-1) \quad \text{or} \\ a_\mathrm{s} &= 2V'-2k-2V'\alpha(2p_\mathrm{l}-1). \end{aligned} \tag{26}$$

In Eq. (26), when $\alpha=0$, the above neutral stability curve can be transformed as

$$a_\mathrm{s} = 2V'-2k. \tag{27}$$

The above curve is consistent with the conclusion in the literature.[74] Therefore, the heterogeneous traffic flow model proposed in this paper can be regarded as a generalized form of the traditional homogeneous traffic flow model.

Figure 1(a) shows the neutral stability curve under different values of penetration rate of drivers with low intensity $q$, where the apex of the curve represents the critical point. The entire phase space is subdivided into two parts by this curve. The area above the curve is the stability region, while the area below the curve is an unstable region. As the value of parameter $q$ increases, the critical point of the curve rises, such that the entire stability area is compressed and the traffic flow stability is weakened. Figure 1(b) shows the corresponding relationship between the critical point and the parameter $q$. As we can see, as the value of parameter $q$ increases, the critical point also shows an increasing trend. This conclusion also explains Fig. 1(a).

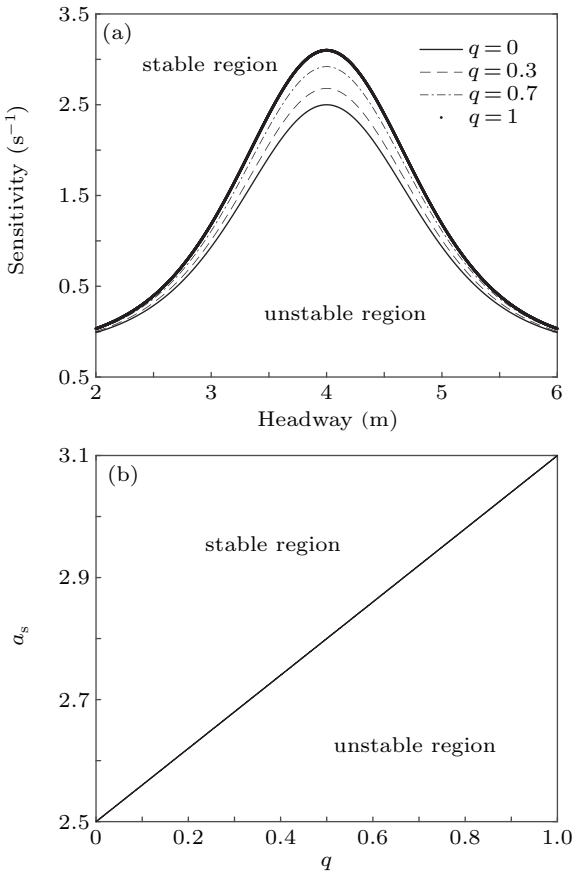



**Fig. 1.** (a) Neutral stability curves under different values of the parameter $p$. (b) Critical point $a_\mathrm{s}$ against the parameter $p$, where $p_\mathrm{l}=0.3$, $p_\mathrm{h}=0.7$, $\alpha=0.25$, and $k=0.1$.

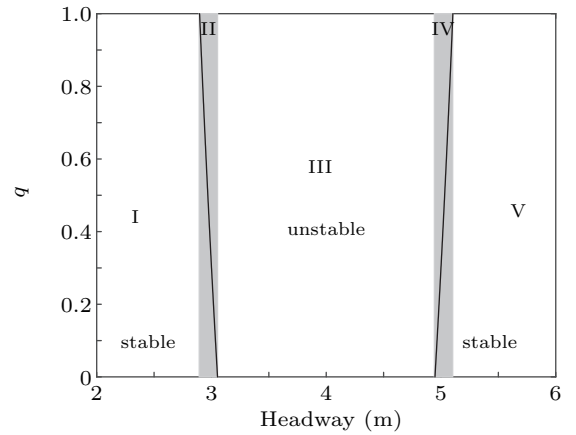



**Fig. 2.** The space $(y,p)$ divided into five distinct regions by the critical curve.

In order to better quantify the relationship between the parameter $q$ and the headway $y$, the neutral stability curve is simplified as follows:

$$q = \frac{2V'-a-2k-2\alpha(2p_\mathrm{h}-1)V'}{4\alpha V'(p_\mathrm{l}-p_\mathrm{h})}. \tag{28}$$

Figure 2 shows the neutral stability curve in the phase space $(y,p)$. As we can see, the entire phase space is divided into five regions by the neutral curve. In the high-density region I and the low-density region IV, the heterogeneous traffic flow satisfies the stability regardless of the value of coefficient

$p$. When the headway $\Delta x$ falls into regions II and IV, as the parameter $p$ increases, the stability of the heterogeneous traffic flow is weakened. When the headway $\Delta x$ falls into region III, the stability of the heterogeneous traffic flow is not satisfied regardless of the value of the coefficient $p$, such that any small disturbance will evolve into a traffic jam.

In the literature, the impact of heterogeneity and traffic flow stability was analyzed by simulation, whereas no evidence on analytical results has been provided. To address this issue, we assume that the penetration rate of drivers with low intensity parameter of driver's characteristics is half, i.e., $q = 1/2$, and introduce the following variables:

$$p_{\mathrm{a}} = \frac{1}{2}\left(p_{\mathrm{l}} + p_{\mathrm{h}}\right),$$
$$\Delta p = \sqrt{\frac{1}{N}\sum_{i=1}^{N}\left(p_i - p_{\mathrm{a}}\right)} = p_{\mathrm{a}} - p_{\mathrm{l}} = p_{\mathrm{h}} - p_{\mathrm{a}}, \tag{29}$$

where $p_{\mathrm{a}}$ is the average value of two intensity parameter of driver's characteristics $p_{\mathrm{l}}$ and $p_{\mathrm{h}}$, and $\Delta p$ is the standard deviation of all drivers.

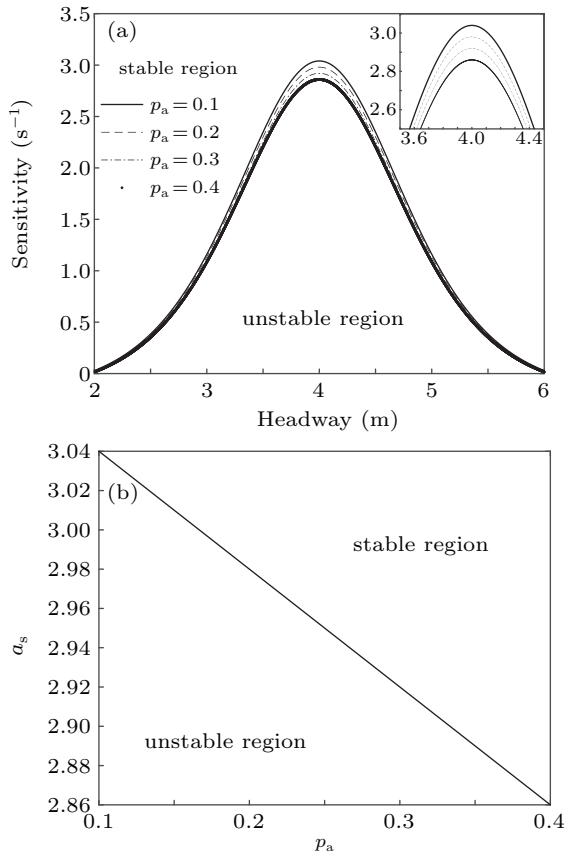



**Fig. 3.** (a) Neutral stability curves under different values of the parameter $p_{\mathrm{a}}$. (b) Critical point $a_{\mathrm{s}}$ against the parameter $p_{\mathrm{a}}$, where $\alpha = 0.1$, $k = 0.1$, and $\Delta p = 0.1$.

Substituting Eq. (29) into Eq. (25), the following new neutral stability curve can be obtained:

$$\begin{aligned} a_{\mathrm{s}} \;=\; & 2V' - 2k - V'\alpha\left[2\left(p_{\mathrm{a}} - \Delta p\right) - 1\right] \\ & - V'\alpha\left[2\left(p_{\mathrm{a}} + \Delta p\right) - 1\right]. \end{aligned} \tag{30}$$

Figures 3 and 4 present the effect of the average value $p_{\mathrm{a}}$ and standard deviation $\Delta p$ on the traffic flow stability, respectively. We can see that the effects of these two parameters on traffic flow stability are quite distinct. More specifically, as the value of parameter $p_{\mathrm{a}}$ increases, the critical point of the curve reduces and the area of the stability area expands, which indicates that the stability of traffic flow is enhanced. As shown in Fig. 4, the change of neutral stability curve is trivial as the parameter $\Delta p$ increases, and that the critical point is nearly an constant (Fig. 4(b)).

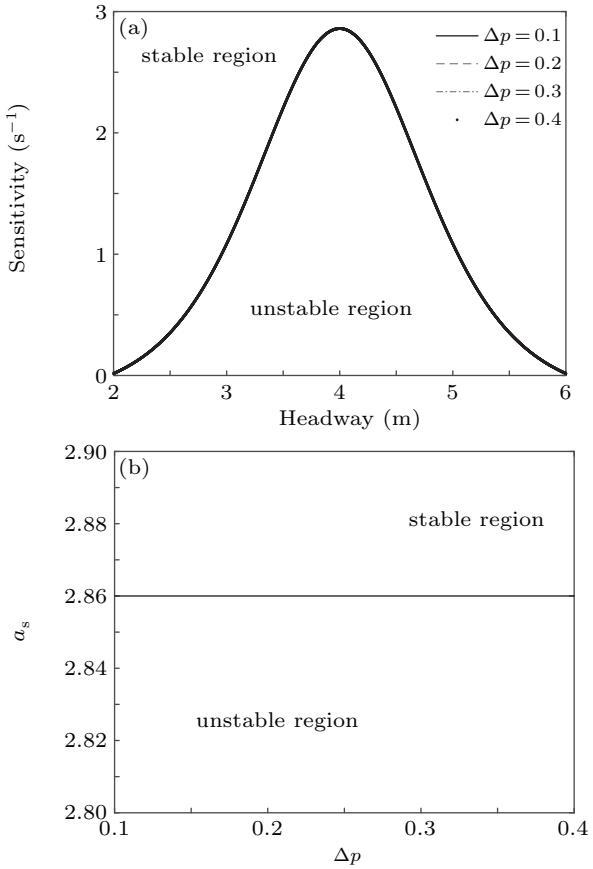



**Fig. 4.** (a) Neutral stability curves under different values of the parameter$\Delta p$. (b) Critical point $a_{\mathrm{s}}$ against the parameter $\Delta p$, where $\alpha = 0.1$, $k = 0.1$, and $p_{\mathrm{a}} = 0.4$.

## 4. Simulation example

In this section, simulation is conducted to verify the linear stability analysis. We assume that all vehicles are running along a single lane under periodic boundary conditions, and the initial conditions of the proposed model are taken as follows:

$$\begin{aligned} & y_i(0) = y_i(1) = y_0, \qquad \left(i \neq \tfrac{N}{2}, \tfrac{N}{2}+1\right), \\ & y_i(0) = y_i(1) = y_0 - \delta, \ \left(i = \tfrac{N}{2}\right), \\ & y_i(0) = y_i(1) = y_0 + \delta, \ \left(i = \tfrac{N}{2}+1\right), \\ & v_n^0 = V\left(y_0\right). \end{aligned} \tag{31}$$

In order to better compare with the Peng's model,[47] the key parameters are borrowed from the literature.[47] More

specifically, the average headway $y_0 = 4$, the number of vehicles $N = 100$, the initial disturbance $\delta = 0.5$, and the driver's sensitivity $a = 2.58$. In order to obtain a less biased result, the effect of the vehicle positions should be eliminated. To this end, we randomly distribute $pN$ drivers with low intensity parameter of driver's characteristics in the platoon.

### 4.1. Impact of penetration rate

Figure 5 shows the spatiotemporal evolution of vehicle velocity under different values of penetration rate of drivers with low intensity, $q$. When $q = 0$, there are only aggressive drivers and the traffic flow is relatively stable. As the parameter $q$ increases, two types of drivers coexist along the road and their interactions become more evident, such that the traffic flow is more fluctuated. When parameters $q$ increases to 1, all drivers become timid and the traffic fluctuation becomes worst. These results suggest that the provision of aggressive drivers contribute to the traffic flow stability, whereas the provision of timid drivers has a negative impact on the traffic flow stability. This is due to the fact that the aggressive drivers tend to preemptively adjust the speeds that prepare the system for delays. Figure 6 shows the instantaneous velocity distribution corresponding to Fig. 5, from which we found that as the parameter $q$ increases, the amplitude of vehicle velocity fluctuation gradually increases. This result matches the above conclusion from Fig. 5.

Figure 7 shows the hysteresis loop curves under different values of the parameter $q$. The relationship between the parameter $q$ and the traffic flow stability can be explored based on the area enclosed by the curve. Generally, a larger area indicates the more unstable traffic flow. As we can see, as the parameter $q$ increases, the area enclosed by the hysteresis loop curve expands, which indicates that the traffic flow stability is stronger. This result agrees with Figs. 5–7. Therefore, it is concluded that the penetration rate $q$ contributes negatively to the stability of the traffic flow.

### 4.2. Impact of average value $p_a$ and standard deviation $\Delta p$

In order to analyze the effect of driver heterogeneity characteristic on the traffic flow stability, in what follows we analyze the relationship between the average value $p_a$ and the standard deviation $\Delta p$ of two intensity parameters characterizing two types of drivers and the traffic flow stability. Figures 8–10 depict the effect of average value $p_a$ on the traffic flow stability. As the parameters $p_a$ increases, the interaction between vehicles is weakened, and the fluctuation amplitude of velocity is gradually reduced. Accordingly, the area enclosed by the hysteresis loop curve gradually decreases. Therefore, a higher parameter $p_a$ can improve the traffic flow stability, which is consistent with the conclusion in the literature.[47]

Figures 11–13 depict the effect of the standard deviation $\Delta p$ on the heterogeneity traffic flow stability. As we can see, given the average value $p_a$, the change of velocity fluctuating amplitudes and hysteresis loop curves are trivial as the standard deviation $\Delta p$ increases. Therefore, compared to the effect of average value $p_a$, the effect of the standard deviation $\Delta p$ on the stability of traffic flow is trivial.

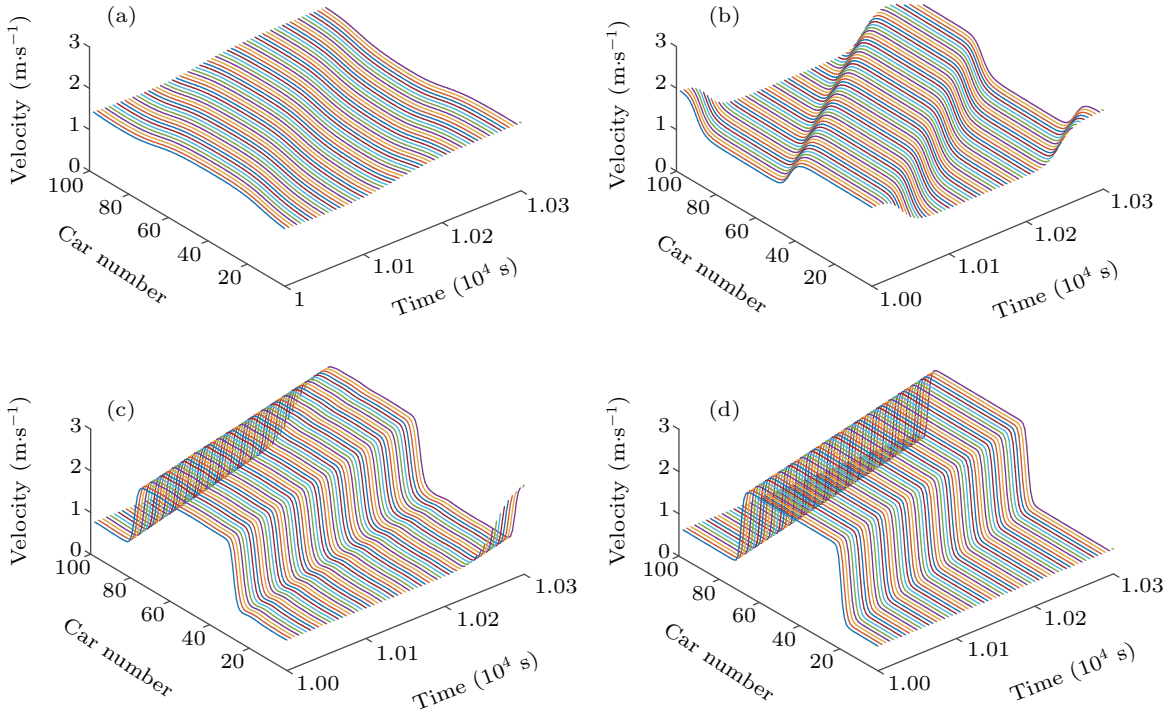



**Fig. 5.** Spatiotemporal evolution profiles of vehicle velocity under different values of the parameter $q$, (a) $q$ =0; (b) $q$ =0.3; (c) $q$ =0.7; (d) $q$ =1, where $p_l = 0.3$, $p_h = 0.7$, $k$ =0.1, $\alpha = 0.1$.

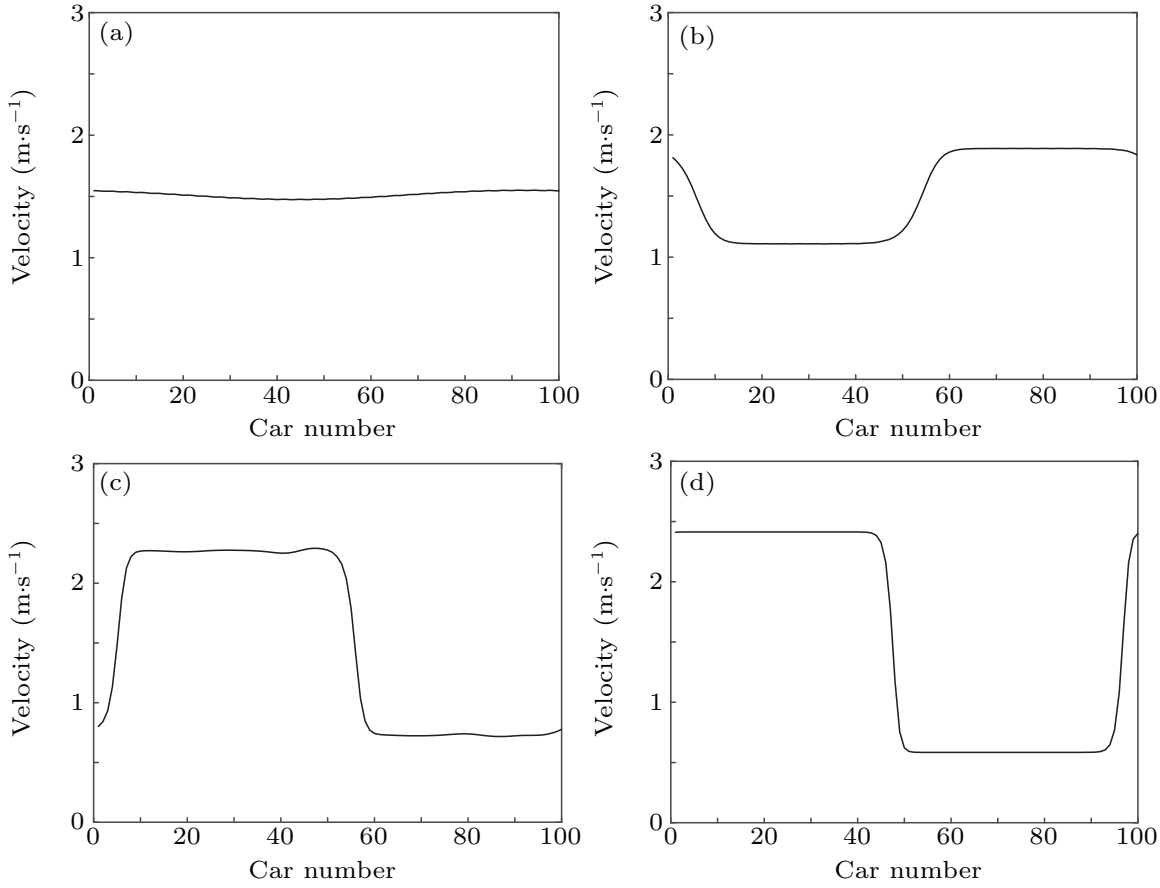



**Fig. 6.** The instantaneous velocity distribution corresponding to Fig. 5.

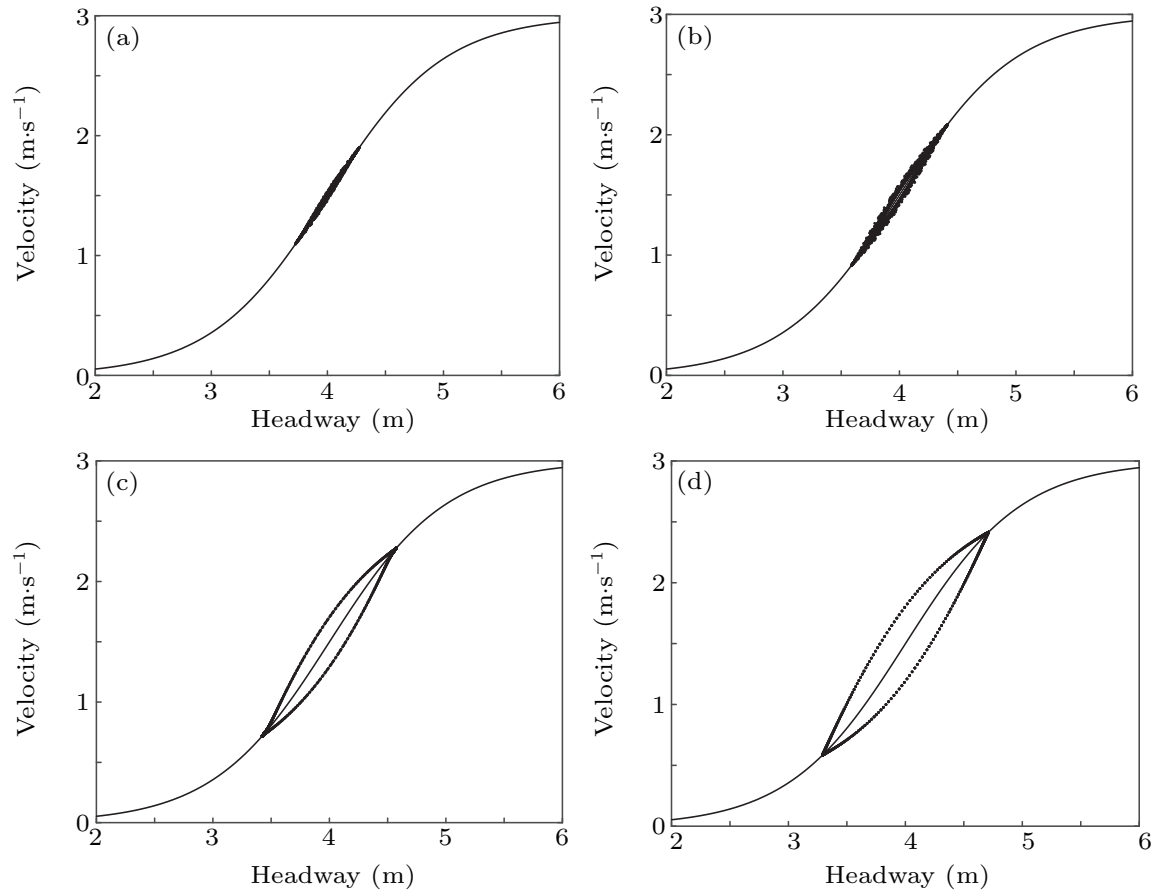



**Fig. 7.** Hysteresis loop curves of mid-position vehicle corresponding to Fig. 5.

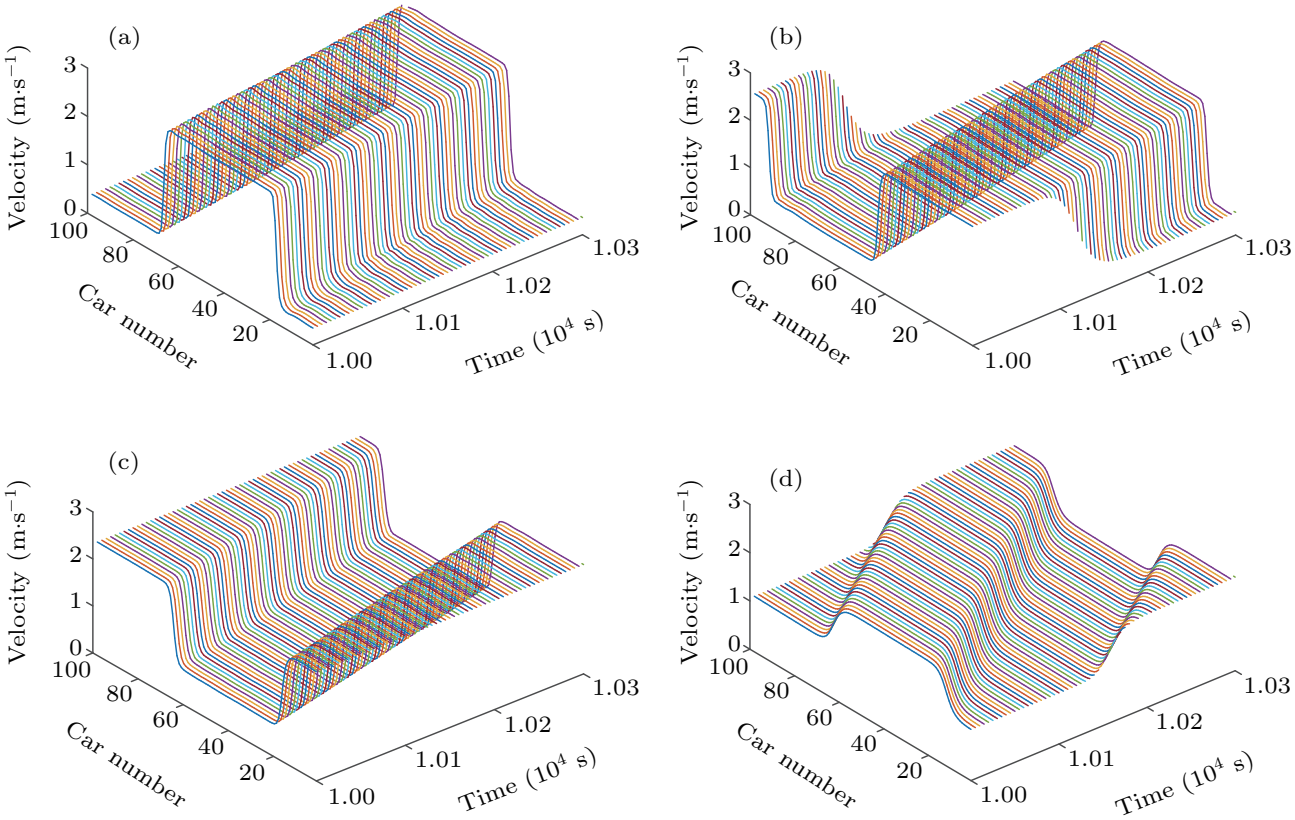



**Fig. 8.** Time evolutions of velocity profiles under different values of the parameter $p_a$, (a) $p_a = 0.1$; (b) $p_a = 0.2$; (c) $p_a = 0.3$; (d) $p_a = 0.4$, where $\Delta p = 0.1$, $k = 0.3$, $\alpha = 0.2$, and $q = 0.5$.

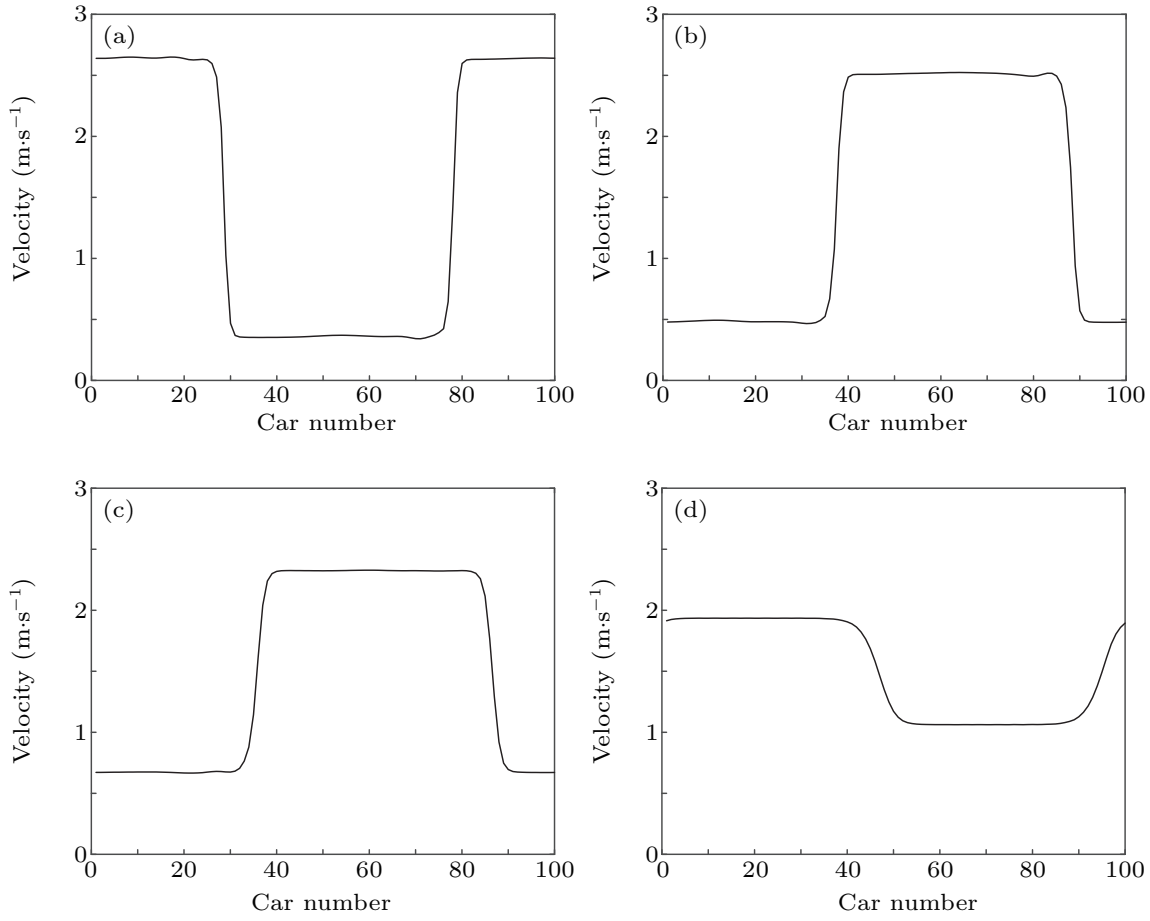



**Fig. 9.** The instantaneous velocity distribution corresponding to Fig. 8.

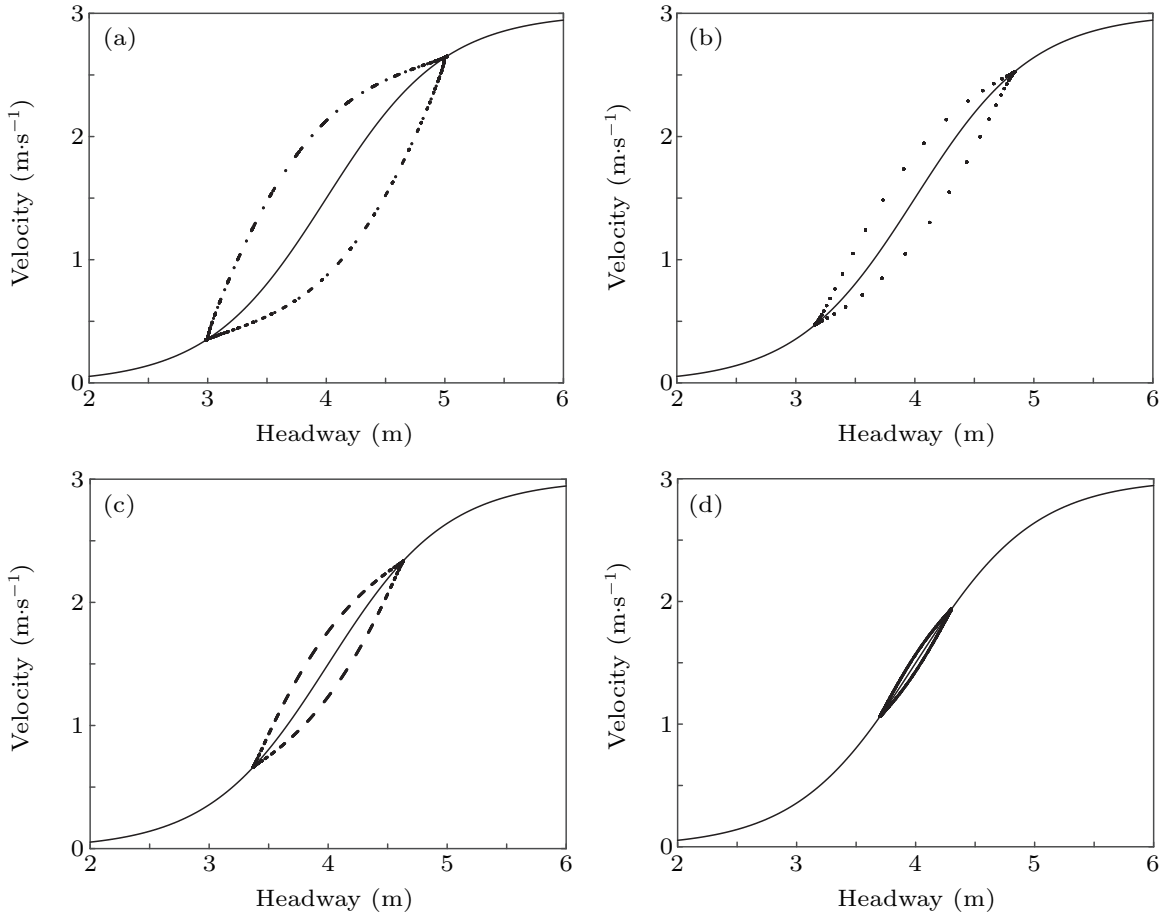



**Fig. 10.** The hysteresis loop curves of mid-position vehicles corresponding to Fig. 8.

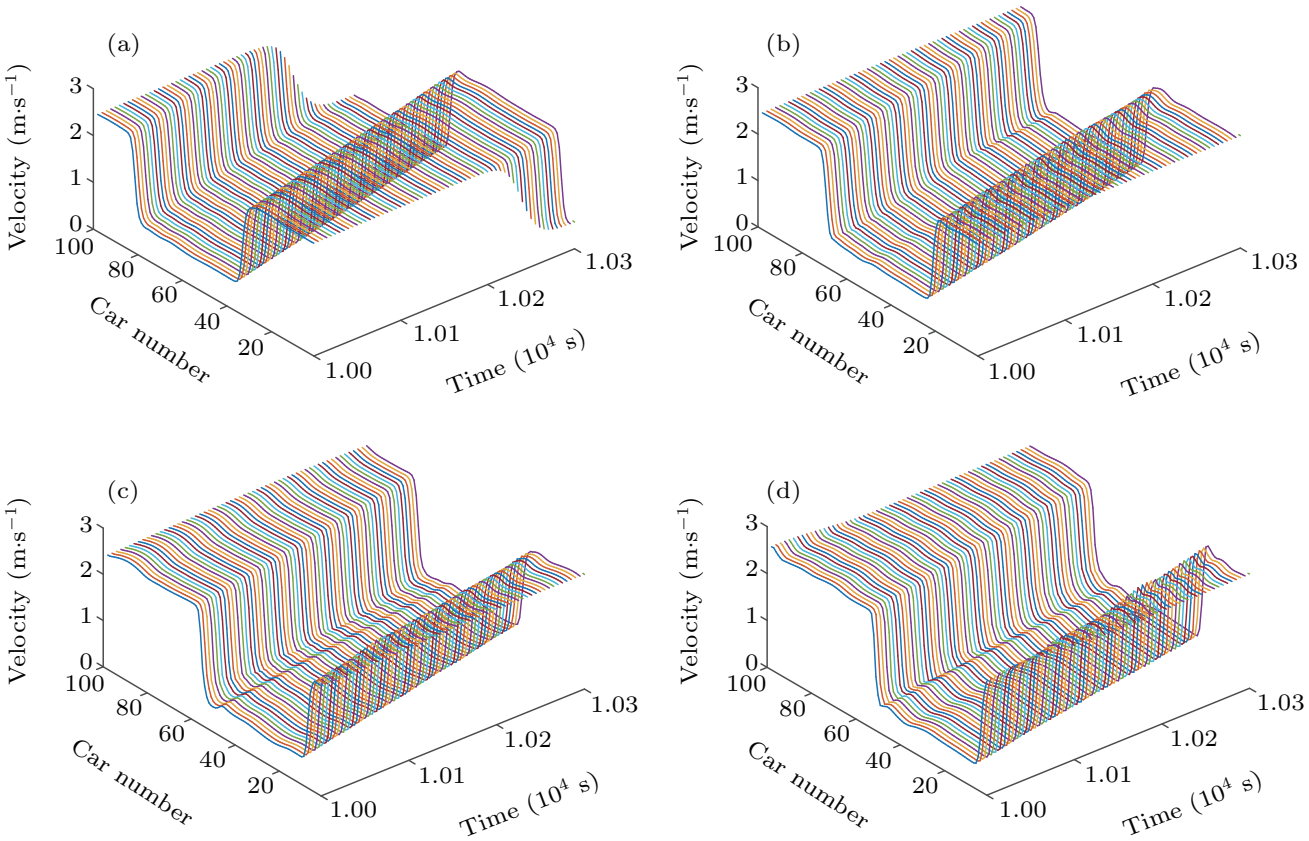



**Fig. 11.** Time evolutions of velocity profiles under different values of the parameter $\Delta p$, (a) $\Delta p = 0.1$; (b) $\Delta p = 0.2$; (c) $\Delta p = 0.3$; (d) $\Delta p = 0.4$, where $p_a = 0.4$, $k = 0.1$, $\alpha = 0.2$, and $q = 0.5$.

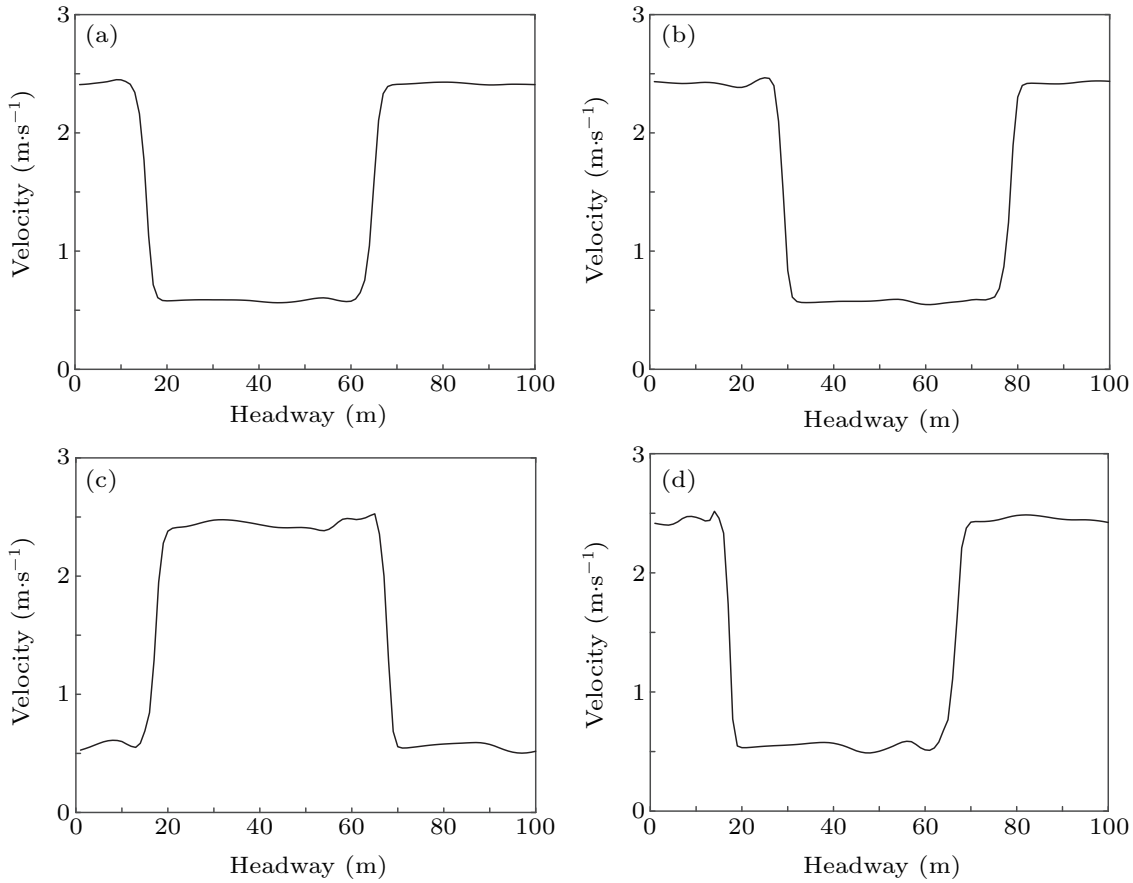



**Fig. 12.** The instantaneous velocity distribution corresponding to Fig. 11.

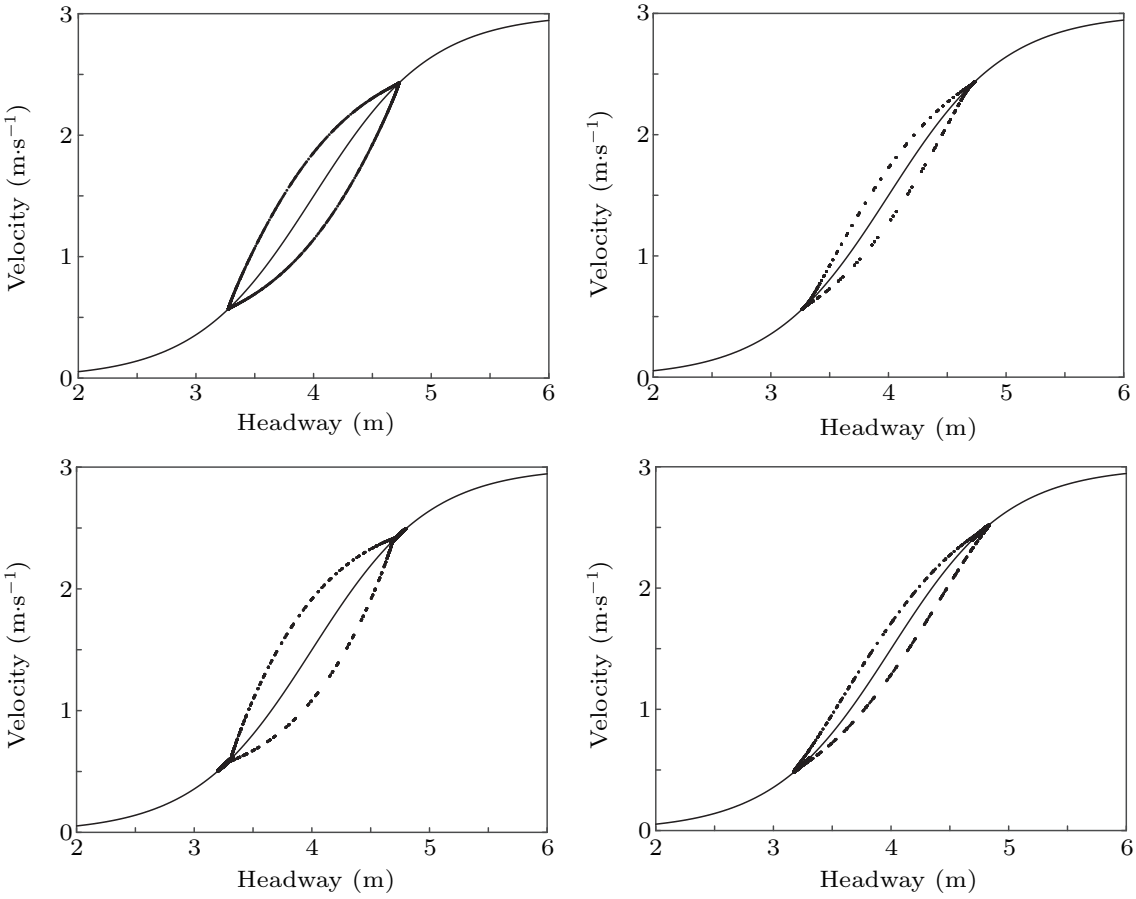



**Fig. 13.** The hysteresis loop curves of mid-position vehicles corresponding to Fig. 11.

## 5. Conclusion

In this paper, we proposed a new car-following model for heterogeneous traffic flow with timid and aggressive drivers. In the linear stability analysis, we obtained the stability conditions of the proposed heterogeneous traffic flow model. The neural stability diagram with five distinct regions was also derived. Simulation results showed that the traffic flow stability decreases as the penetration rate of timid drivers increases, which suggests that the provision of timid drivers contributes negatively to the stability of traffic flow. The effect of driver heterogeneous characteristics on the stability of traffic flow was explored through the average value and standard deviation of intensity parameters characterizing two types of drivers. Results showed that the average value has a great impact on the stability of traffic flow, whereas the impact of the standard deviation is trivial.

To the best of the authors' knowledge, this is the first paper on heterogeneous traffic flow model with timid and aggressive drivers. This research is expected to provide insights for the traffic simulation and platform development. Future studies can incorporate the effect of vehicle overtaking, merging and leaving of vehicles. In addition, it would be also interesting to incorporate a fine-grained road environment into the heterogeneous traffic flow.

## References


[1] Wu W T, Liu R H, Jin W Z and Ma C X 2019 *Transport. Res. Part B.* **121** 275
[2] Wu W T, Li P, Liu R H, Jin W Z, Yao B Z, Xie Y Q and Ma C X 2020 *Transport. Res. Part E* **142** 102041
[3] Wu W T, Liu R H, Jin W Z and Ma C X 2019 *Transport. Res. Part E.* **130** 61
[4] Wu W T, Lin Y, Liu R H, Li Y H, Zhang Y and Ma C X 2020 *IEEE Trans. Intel. Transport. Systems* 1
[5] Zhai C and Wu W T 2018 *Nonlinear Dynam.* **93** 2185
[6] Zhai C, Liu W M, Tan F G, Huang L and Song M L 2018 *Transport. Plan. Techn.* **39** 801
[7] Zhai C and Wu W T 2019 *Int. J. Mod. Phys. C* **30** 1950073
[8] Ma G Y, Ma M H, Liang S D, Wang Y S and Zhang Y Z 2020 *Commun. Nonlinear Sci.* **85** 105221
[9] Sun Y Q, Ge H X and Cheng R J 2019 *Physica A* **521** 752
[10] Sun Y Q, Ge H X and Cheng R J 2019 *Physica A* **527** 121426
[11] Hua W, Yue Y X, Wei Z L, Cheng J H and Wang W R 2020 *Physica A* **556** 124777
[12] Yang L, Zheng J R, Cheng Y and Ran B 2019 *Physica A* **535** 122277
[13] Li Q L, Wong S C, Min J, Tian S and Wang B H 2016 *Physica A* **456** 128
[14] Gupta A K and Katiyar V K 2007 *Transportmetrica* **3** 73
[15] Gupta A K and Sharma S 2012 *Chin. Phys. B* **21** 015201
[16] Gupta A K and Sharma S 2010 *Chin. Phys. B* **19** 110503
[17] Gupta A K and Dhiman I 2015 *Nonlinear Dynam.* **79** 663
[18] Zhai C and Wu W T 2020 *Commun. Theor. Phys.* **72** 105004
[19] Zhai C and Wu W T 2020 *Eur. Phys. J. B* **93** 52
[20] Gupta A K and Redhu P 2014 *Nonlinear Dynam.* **76** 1001
[21] Redhu P and Gupta A K 2015 *Physica A* **421** 249
[22] Zhai C and Wu W T 2021 *Commun. Nonlinear Sci.* **95** 105667
[23] Zhai C and Wu W T 2020 *Int. J. Mod. Phys. C* **31** 2050089
[24] Gupta A K and Redhu P 2013 *Physica A* **392** 5622
[25] Sharma S 2016 *Nonlinear Dynam.* **86** 2093
[26] Sharma S 2015 *Nonlinear Dynam.* **81** 991
[27] Sharma S 2015 *Physica A* **421** 401
[28] Bando M, Hasebe K, Nakayama A, Shibata A and Sugiyama Y 1995 *Phys. Rev. E* **51** 1035
[29] Zhang J, Tang T Q and Yu S W 2018 *Physica A* **492** 1831
[30] Jin Z Z, Li Z P, Cheng R J and Ge H X 2018 *Physica A* **507** 278
[31] Li S K, Yang L X, Gao Z Y and Li K P 2014 *ISA T.* **53** 1739
[32] Li Y F, Zhong Z Y, Zhang K B and Zheng T X 2019 *Physica A* **533** 122022
[33] Guo L T, Zhao X M, Yu S W, Li X H and Shi Z K 2017 *Physica A* **471** 436
[34] Zhang G, Zhao M, Sun D H, Liu W N and Li H M 2016 *Physica A* **442** 532
[35] Li Y F, Sun D H, Liu W N, Zhang M, Zhao M, Liao X Y and Tang L 2011 *Nonlinear Dynam.* **66** 15
[36] Yu L, Shi Z K and Li T 2014 *Phys. Lett. A* **378** 348
[37] Ge H X, Meng X P, Cheng R J and Lo S M 2011 *Physica A* **390** 3348
[38] Zhu H B and Dai S Q 2008 *Physica A* **387** 3290
[39] Cao B G 2020 *Physica A* **539** 122903
[40] Wang Y J, Song H and Cheng R J 2019 *Physica A* **515** 440
[41] Liu D W, Shi Z K and Ai W H 2017 *Commun. Nonlinear Sci.* **47** 139
[42] Peng G H and Cheng R J 2013 *Physica A* **392** 3563
[43] Zhang J, Wang B, Li S B, Sun T and Wang T 2020 *Physica A* **540** 123171
[44] Cheng J Z, Liu R H, Ngoduy D and Shi Z K 2016 *Nonlinear Dynam.* **85** 2705
[45] Zhou T, Sun D H, Kang Y R, Li H M and Tian C 2014 *Commun. Nonlinear Sci.* **19** 3820
[46] Tang T Q, He J, Yang S C and Shang H Y 2014 *Physica A* **413** 583
[47] Peng G H, He H D and Lu W Z 2016 *Physica A* **442** 197
[48] Cheng R J, Ge H X and Wang J F 2017 *Phys. Lett. A* **381** 1302
[49] Sharma S 2015 *Physica A* **421** 401
[50] Peng G H and Qing L 2016 *Mod. Phy. Lett. B* **30** 1650351
[51] Wang Z H, Ge H X and Cheng R J 2020 *Physica A* **540** 122988
[52] Tang T Q, Luo X F and Liu K 2016 *Physica A* **457** 316
[53] Tang T Q, Li J G, Yang S C and Shang H Y 2015 *Physica A* **419** 293
[54] Ge H X, Meng X P, Zhu H B and Li Z P 2014 *Physica A* **408** 28
[55] Li Y F, Zhang L, Zheng H, He X Z, Peeta S, Zheng T X and Li Y G 2015 *Nonlinear Dynam.* **82** 629
[56] Li Y F, Zhang L, Peeta S, Pan H G, Zheng T X, Li Y G and He X Z 2015 *Nonlinear Dynam.* **80** 227
[57] Li Y F, Zhang L, Zhang B, Zheng T X, Feng H Z and Li Y G 2016 *Nonlinear Dynam.* **85** 1901
[58] Wang P C, Yu G Z, Wu X K, Qin H M and Wang Y P 2018 *Physica A* **496** 351
[59] Sun Y Q, Ge H X and Cheng R J 2019 *Physica A* **534** 122377
[60] Li Y F, Zhang L, Peeta S, He X Z, Zheng T X and Li Y G 2016 *Nonlinear Dynam.* **85** 2115
[61] Yu S W and Shi Z K 2015 *Physica A* **428** 206
[62] Li Y F, Kang Y H, Yang B, Peeta S, Zhang L, Zheng T X and Li Y G 2016 *Physica A* **462** 38
[63] Jin Y F and Hu H Y 2013 *Commun. Nonlinear Sci.* **18** 1027
[64] Chen D, Sun D H, Zhao M, Yang L Y, Zhou T and Xie F 2018 *Nonlinear Dynam.* **92** 1829
[65] Yang D, Qiu X P, Yu Dan, Sun R X and Pu Yun 2015 *Physica A* **424** 62
[66] Li Q L, Wong S C, Jie M, Tian S and Wang B H 2016 *Physica A* **456** 128
[67] Li Z P, Xu X, Xu S Z and Qian Y Q 2017 *Commun. Nonlinear Sci.* **42** 132
[68] Sun F X, Wang J F, Cheng R J and Ge H X 2018 *Phys. Lett. A* **382** 489
[69] Wang J F, Sun F X, Cheng R J and Ge H X 2018 *Physica A* **506** 1113
[70] Li Z P, Li W Z, Xu S Z, Qian Y Q and Sun J 2015 *Physica A* **436** 729
[71] Ren W L, Cheng R J and Ge H X 2021 *Appl. Math. Comput.* **401** 126079
[72] Ren W L, Cheng R J and Ge H X 2021 *Appl. Math. Model.* **94** 369
[73] Helbing D and Tilch B 1998 *Phys. Rev. E* **58** 133
[74] Jiang R, Wu Q S and Zhu Z J 2001 *Phys. Rev. E* **64** 017101